SCOUR AND HYDRODYNAMIC EFFECTS OF DEBRIS BLOCKAGE AT MASONRY BRIDGES: INSIGHTS FROM EXPERIMENTAL AND NUMERICAL MODELLING

MOHSEN EBRAHIMI[1], RECEP KAHRAMAN[2], PRAKASH KRIPAKARAN[3], SLOBODAN DJORDJEVIĆ[4], GAVIN TABOR[5], DUŠAN M. PRODANOVIĆ[6], SCOTT ARTHUR[7] & MATTHEW RIELLA[8]

[1-5, 8] Centre for Water Systems, University of Exeter, Exeter, United Kingdom
M.Ebrahimi@exeter.ac.uk; R.E.Kahraman@exeter.ac.uk; P.Kripakaran@exeter.ac.uk; S.Djordjevic@exeter.ac.uk; G.R.Tabor@exeter.ac.uk; mjr214@exeter.ac.uk

[6] Faculty of Civil Engineering, University of Belgrade, Belgrade, Serbia
dprodanovic@grf.bg.ac.rs

[7] Institute for Infrastructure and Environment, Heriot-Watt University, Edinburgh, United Kingdom
S.Arthur@hw.ac.uk

ABSTRACT

This paper describes preliminary results of a project investigating the scour and hydrodynamic effects of debris blockage at masonry bridges. Debris blockage, which is often cited as one of the primary causes of bridge failures in the UK and around the world, results in a larger obstruction to the flow leading to increased flow velocities, scour and hydrodynamic forces, compared to the conditions without debris. This, in turn, can affect the structural stability of bridges, for example, by undermining their foundations. Masonry bridges, many of which are valuable historical assets, are particularly vulnerable to debris blockage due to their short spans and low clearance. The reported study, being undertaken at the Centre for Water Systems at the University of Exeter, has two main phases: (i) laboratory experiments and (ii) CFD simulations. In the first phase, a 0.6m-wide and 10m-long flume is utilized to study the flow hydrodynamics and scour associated with pier/bridge models in several reference scenarios. The geometry of the pier/bridge and debris models are kept approximately similar to prototype conditions, with hydraulic conditions of the experiments designed to the degree that laboratory constraints allow to maintain Froude similarity. Velocities and scour are measured via an acoustic Doppler velocimeter and echo-sounding concept. Experimental results are used to calibrate and validate CFD models which can later enable simulation of more complicated scenarios. This paper will report these preliminary results from both experimental and CFD phases. Preliminary experimental results highlight the significance of debris existence in enhancing scour due to increasing flow downward velocities. Preliminary results from CFD modelling also show good agreement with experimental results.

Keywords: Debris blockage; masonry bridges, scour, laboratory experiments, CFD.

1 INTRODUCTION

Debris has been acknowledged for many years as a major factor affecting the risk of bridge failure during floods (Laursen and Torch, 1956; Chang and Shen, 1979; Diehl, 1997; Parola et al., 2000). It increases the effective width of a pier and constricts flow, thereby reducing conveyance and increasing water levels at the pier/bridge. These effects, in turn, enhance the hydraulic loading on structures such as culverts, bridge piers and abutments, and worsen scour (e.g. May et al., 2002; Bradley et al., 2005; McKibbins et al., 2006; Lagasse et al., 2010; Wallerstein et al., 2010; Arneson et al., 2012; Benn, 2013). Masonry bridges, which constitute 40% of the UK bridge stock (Bridle and Sim, 2009), are particularly vulnerable to debris blockage due to their special geometry that typically includes short spans and low clearances. The majority of masonry bridges, including a significant number classified as cultural and engineering heritage structures, were designed hundreds of years ago to withstand flood events less severe and less frequent than those happening today (RSSB, 2005). Consequently, during the flood events of the past decade such as those due to the storms (e.g. Storms Desmond and Frank) of winter 2015/16, hundreds of masonry bridges suffered significant damage with a few even taken to total collapse.

Despite recognising the role of debris in increasing the risk of bridge failure, the current UK guidance for assessment of bridge structures under hydraulic action (May et al., 2002; Highway Agency, 2012; Kirby et al. 2015) fails to provide a reliable approach for accounting for the scour and hydrodynamic effects of debris blockage. Presently the commonly adopted approach to predict scour due to debris blockage is by increasing pier width based on the original “effective pier width” concept of Melville and Dongol (1992). This concept substitutes debris and original pier with a pier with an increased width and does not explain the explicit effect of debris on flow hydrodynamics. However, while still recommended in the recently revised CIRIA manual for evaluating scour at bridges (Kirby et al., 2015), this approach is known to overestimate effective pier width (Lagasse et al., 2010). The current project is aimed at improving this approach at next stages.

Previous research on pier scour due to debris is limited to pier geometries or pier arrangements which are not representative of masonry bridges (e.g. Pagliara and Carnacina 2011, 2013). Also, available investigations have mainly focused on single pier and not the whole bridge (e.g. Lagasse et al. 2010). This is particularly important considering the significant number of failures of single span structures on small watercourses due to abutment scour (Benn, 2013). Therefore, there is a pressing need for scientific research to fill the knowledge gaps with respect to the hydrodynamic effects of debris blockage. Accordingly, a project was defined to investigate the effects of debris blockage on flow pattern, scour and hydrodynamic loads at masonry bridges under flood conditions. This project has three phases: (i) Flume experiments, (ii) CFD simulation, and (iii) Assessment guidance development. The goal of the first phase is to test reference scenarios of flow, debris and structure combinations to provide data for the development of numerical models and their validation in the second phase, i.e. CFD simulations. Scenarios at full-scale with real-life hydraulic conditions will then be simulated via developed CFD codes, and results from both phases will be used to develop an assessment guidance in the third phase of the project. Project outcomes will be built into the existing UK guidance (Kirby et al. 2015) for assessment of bridges under hydraulic action, and is expected to enable improved management of bridges at risk to debris blockage. A detailed review of the project background and methodology is presented in Ebrahimi et al. (2016). The present paper reports on preliminary results from flume experiments and CFD simulations.

2 FLUME EXPERIMENTS

Flume experiments were carried out in a sediment recirculating flume that is 0.6m-wide, 0.65m-deep and with a 10m-long working section. The flume is equipped with a 3-axis traverse system for positioning instruments at predefined (x, y, z) coordinates, with x, y and z being streamwise, cross stream and vertical directions. Flume experiments are designed to understand the effect of simple cylindrical debris on flow hydrodynamics and scour around a single pier. The flume's relatively small width does not allow for scaling down of all relevant hydraulic quantities such as pier geometry and sediment size proportionately. However experimental scenarios are still suitably representative of real conditions, and sufficiently varied to support CFD validation, which is the main purpose of the experiments.

2.1 Hydraulic conditions

The hydraulic conditions for the experiments discussed in this paper are summarized in Table 1. Experiments 1-2 were carried out to investigate only scour, while in experiments 3-4 both flow hydrodynamics and scour were measured (see subsections 2.3 and 2.4). In the table, B = flow width, d_{50} = average grain diameter of sediment, h = approach flow depth, Q = flow rate, R = flow Reynolds number (= Vh/ν, with V = Q/(Bh) and ν being the mean flow velocity and fluid kinematic viscosity, respectively), F = Froude number (= $V/(gh)^{1/2}$, where g stands for acceleration due to gravity), R_* = roughness Reynolds number (= $v_* k_s/\nu$, with v_* = $(gSR_h)^{1/2}$ as shear velocity, where S and R_h stand for longitudinal slope of the bed and hydraulic radius, respectively, and $k_s = 2d_{50}$ is granular roughness, Kamphuis, 1974), and V_{cr} = critical mean flow velocity for initiation of sediment motion (calculated as $V_{cr} = V/\eta_*^{1/2}$, where η_* is flow intensity calculated according to Yalin and da Silva, 2001). L_D and D_D are length and diameter of cylindrical debris.

Table 1. Hydraulic conditions of experiments at present paper (B = 60 cm, d_{50} = 1.37 mm).

Experiment	Approach flow depth ± 0.05 h (cm)	Discharge ± 0.1 Q (l/s)	R	F	R_*	V/V_{cr}	Debris Shape	Debris Length L_D (cm)	Debris Diameter D_D (cm)
1	7.9	19	31673	0.46	78.5	0.95	Cylindrical	30	1.9
2	7.9	19	31673	0.46	78.5	0.95	Cylindrical	30	3.2
3	13.1	35	58349	0.39	81.9	0.99	No debris	-	-
4	13.1	35	58349	0.39	81.9	0.99	Cylindrical	30	3.2

Reynolds number scaling is relaxed while keeping the flow turbulent (R > 2000-3000, Chanson, 2004). In addition, instead of having strict Froude similitude between model and prototype, flow is generally kept subcritical (F < 1). In all tests, the flow is uniform, and in fully rough regime of turbulent flow (R_* > 70, Yalin 1992, Yalin and da Silva 2001). Experiments are carried out in clear-water scour conditions with V/V_{cr} being close to 1 in order to maximize scour depth.

Sediment in the current experiments is uniform silica sand with average grain diameter d_{50} = 1.37 mm and uniformity coefficient d_{60}/d_{10} = 1.37. d_{50} was identified based on

- Having a rough turbulent flow (R* > 70);
- Avoiding ripple forming sand (d50 < 0.6-0.7 mm, Raudkivi and Ettema, 1983; Ettema et al., 1998);
- Availability of the grain size on the market.

A compacted sand bed with sufficient thickness (based on the scour estimate, see Ebrahimi et al., 2016) was then installed in the flume. In order to maximize the number of experiments, duration of each experiment was 5 hours. While this is not sufficient for reaching equilibrium scour depth (Melville and Chiew, 1999), since all

experiments with and without debris were run for the same duration, the results enable quantifying the effect of debris on scour, which is the central aim of this project.

2.2 Scaled models

As shown in the plan view schematic presented in Figure 1, the scaled single pier features two triangular cutwaters which are a typical feature of masonry bridges in the UK. Each cutwater is an isosceles triangle with base angle 45°. A pier width of 50 mm was chosen. This is much less than 1/6th of the flume width (B = 600 mm), the maximum pier size recommended for experiments to avoid adverse effects of side walls (Frostick et al., 2011). Pier streamwise length is 156 mm resulting in a width-to-length ratio of 0.32 that matches the average aspect ratio estimated for several masonry bridge piers mainly in Devon, UK (personal communication with Devon County Council, 2015).

Debris shapes, dimensions and types can vary from one stream to another in practice. However, to begin with, scaled debris in the experiments were represented with simple cylindrical elements representing a tree trunk without rootwads. Although strict scaling of debris was not required in the experiments, a sensible diameter/length ratio of cylindrical debris D_D/L_D was kept near 0.059 which is the average of the diameter/length ratios suggested by several field studies in US, Germany and Italy (Beechie and Sibley, 1997; Diehl, 1997; Kail, 2003; Comiti et al., 2006; Magilligan et al., 2008). The debris length, L_D , was 30 cm (covering half of the flow width) and diameter, D_D, was 1.9 cm. Also, an additional scenario with L_D = 30 cm and D_D = 3.2 cm was used to quantify the effect of cylindrical debris diameter on scour. Cylindrical debris was fixed to the pier cutwater nose just below the free surface of approach flow (Figure 1). Debris was fabricated by 3D printing using nylon powder. This is thought to be a useful technique to fabricate more complicated debris shapes in the next stages of the project.

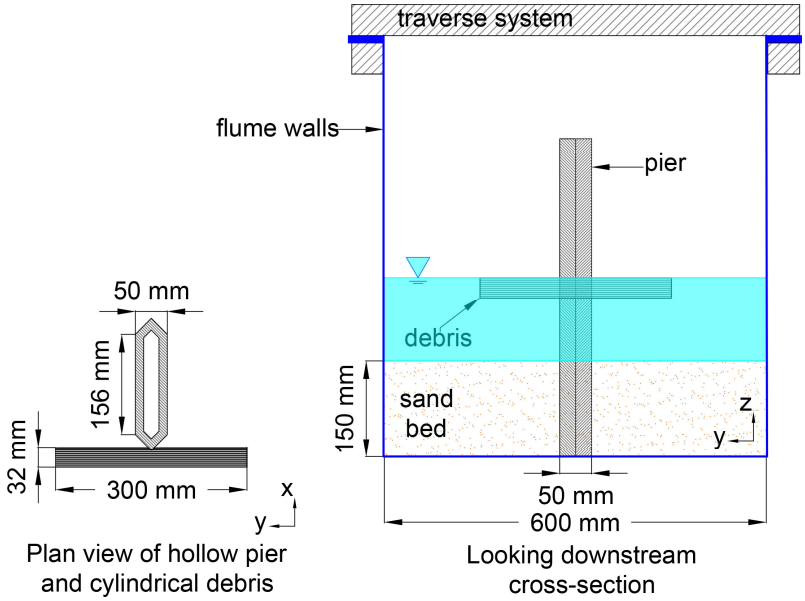

Figure 1. Schematics of experiment 5: Left. Plan view (x shows flow direction); Right. Cross-section.

2.3 Measurements

The flow rate was measured using an electromagnetic flowmeter (resolution ±0.1 l/s) installed in the suction pipe of the centrifugal pump. Approach flow depth was quantified using a digital point gauge (resolution 0.01 mm) mounted sufficiently upstream the pier to read undisturbed free surface elevation. During a 5-hour experiment, mean deviation of free surface elevation from its average was 0.5 mm (see Table 1).

Initial flow velocity field was measured only in experiments 3 and 4 and without any sediment in the flume. Therefore, bed roughness was different in flow experiments and the corresponding scour experiments. However, this was envisaged to be useful for investigating overall effect of debris on flow pattern and providing validation data for CFD modelling. Velocity measurements were carried out with the aid of a Vectrino Profiler ADV (accuracy 0.5% of measured velocity), installed on the 3-axis traverse system. Velocity measurements were performed on a grid of 20 predefined (x, y, z) coordinates. Velocity data collection duration at each point was between 3-20 minutes depending on the degree of turbulence and velocity fluctuations at that point.

Final scour geometry was measured after stopping the flow carefully to avoid any disturbance to the scour topography. Measurements were carried out using the distance measurement feature of ADV probe (accuracy of 0.5 mm) by moving the probe over a grid of ~ 240 predefined (x, y) points at one side of the flume (due to symmetry). Near the pier boundaries where ADV was unable to measure bed distance, additional points were measured manually using the point gauge. The scour topography, a sample of which is shown in Figure 2, was then produced by putting the measured distances together.

2.4 Results

In this section, scour results are presented first. Afterwards, velocity pattern, as the scour underlying process, is discussed.

2.4.1 Scour

Maps of scour final topography in experiments 1-4 are illustrated in Figure 2a-d. Maximum scour, $d_{s,max}$, was invariably located at the side edges of upstream cutwater marked by the yellow line. As can be seen, in high flow depth, i.e. tests 3 & 4, maximum scour increased from 95.7 mm to 112 mm, i.e. 17% increase. Also in low flow depth, maximum scour increased from 78.7 mm in test 1 to 87.8 mm in test 2, corresponding to 11.5%. In other words, for tested debris sizes, existence of debris has a higher effect on scour compared to that of debris dimensions. Role of debris in enhancing scour can be explained by analysing velocity pattern which is presented in Subsection 2.4.2.

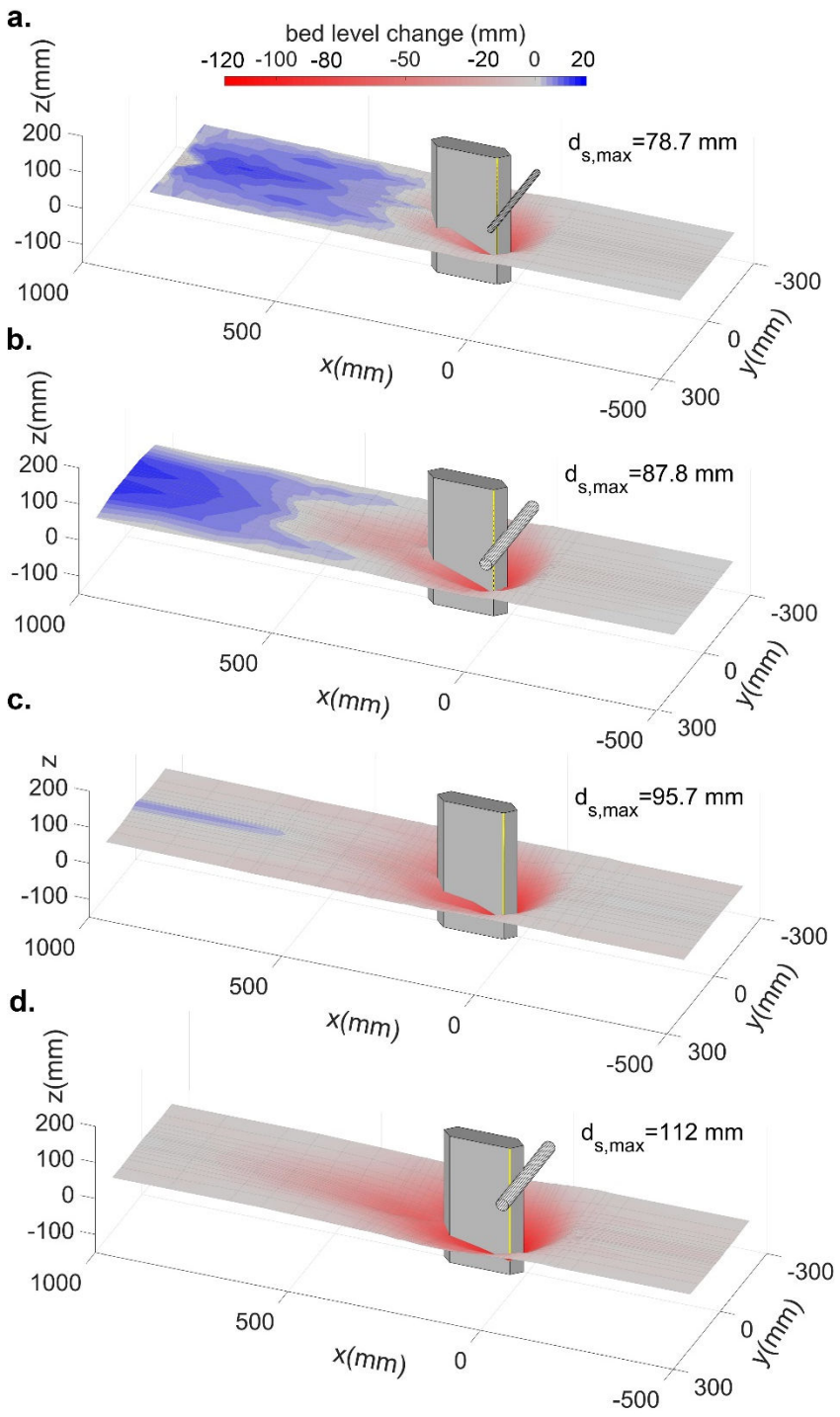

Figure 2. Maps of scour final topography: Experiments 1-5 (a-e). Yellow line marks location of maximum scour depth $d_{s,max}$.

2.4.2 Velocity

In order to have an overall picture of the flow pattern, initial velocity vector fields corresponding to experiments 3 and 4 are shown in Figure 3. It should be noted that velocity measurements were carried out without any sand in the flume and so with different roughness compared to scour experiments. Velocities were measured at twenty nodes in x-y plane numerated 1 to 20 by red colour (Figure 3a) and with resolution ~1 mm in vertical direction. Some of the nodes and vectors are removed for better visibility. Also velocities closer than ~4 cm to the free surface and ~1.5 cm to the bed were not measurable with the utilized instrument.

As can be seen overall velocity fields look similar in experiments 3 and 4. Velocity patterns upstream from the pier (e.g. node 1) are more or less similar in both cases. Downstream from the pier (e.g. nodes 14 and 16), velocities are significantly smaller due to the blocking effect of pier and, as expected, this effect is somewhat larger in the case with debris. Flow acceleration can be seen beside the pier (e.g. nodes 9 and 10) which is due to the narrowing effect of the pier on cross-section and this effect is somewhat larger in the case with debris.

A closer look at vertical velocity components reveals effect of debris in enhancing scour that was described in Subsection 2.4.1. As noted by many researchers (e.g. Hjulström, 1939; Yalin, 1992; van Rijn 1993 amongst others), vertical velocities can affect sediment movement significantly. Vertical component of velocity would loosen and lift sediment while horizontal velocity components remove sediment downstream. Here, this scour enhancing effect is demonstrated by analysing vertical velocities upstream the pier nose in experiments 3 and 4 as shown in Figure 4. In this figure, vertical velocities, i.e. w along z, are exaggerated five times for better visibility. According to the observation by the authors during the experiments, scour initiated at upstream cutwater of the pier. The closest nodes to the pier upstream being common in experiments 3 and 4 are nodes 3-5. In Figure 4, velocities at these nodes are compared between the two experiments. As shown, longitudinal velocities, i.e. u along x, are within the same order; but vertical velocities are substantially larger in experiment 4 with debris. Debris not only partially blocked the cross-section but also diverged the flow toward the bed and increased vertical velocities. Mean values of vertical velocity at all three nodes, calculated by averaging vertical velocities over the whole velocity profile, were similar and ~ -0.85 and -2.5 cm/s at experiments 3 and 4, respectively.

In other words, debris resulted in increased downward velocities ~ 2.9 times on average throughout the whole velocity profile. This enhancement was between 1.2 and 6.4 times with an increasing trend toward the upper border of the measured profile. It is expected that vertical velocities at higher elevations which are closer to debris are affected more than velocities at lower elevations. Consequently, it is expected that in shallower flow, near-bed elevations see higher effect of debris compared to a deeper flow, and so larger enhancement of scour. This will be investigated in the next stage of the current project.

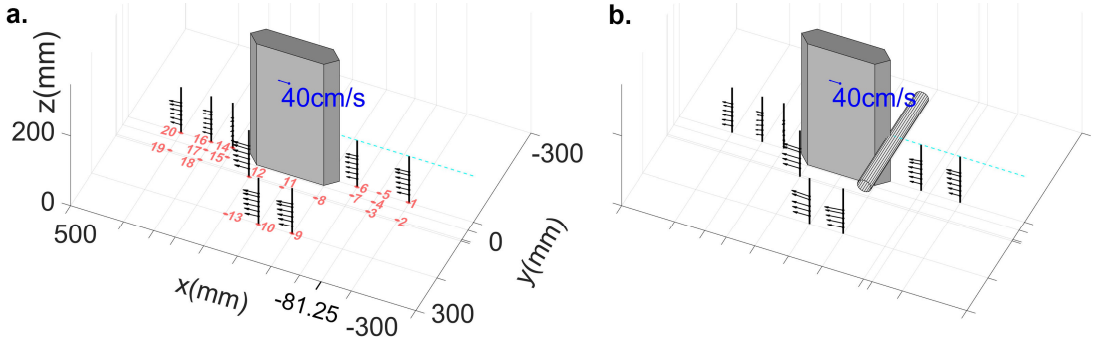

Figure 3. Initial velocity fields in tests 3 (a) & 4 (b). Velocities were measured at nodes numerated by red. Dash line represent free surface elevation & blue vector is reference.

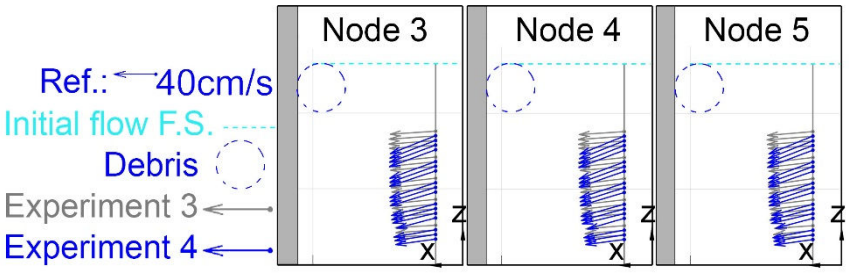

Figure 4. Velocity vectors in x-z plane in experiments 3 and 4 at nodes 3-5 (x = -81.25 mm). Velocity components along z are exaggerated five times for better visibility.

3 CFD SIMULATIONS

3.1 Model description

Throughout this work Computational Fluid Dynamics (CFD) is utilised to effectively model the experimental conditions found within the flume. The Unsteady Reynolds Averaged Navier-Stokes (URANS) equations governing fluid flow are solved numerically using the open-source CFD toolbox, OpenFOAM. OpenFOAM is developed based on the Finite Volume Method (FVM). The FVM is used for describing and evaluating the partial differential equation in form of algebraic linear equations. OpenFOAM includes various modelling capabilities, e.g. multiphase flow. There are several methods such as Mixture, Euler-Euler and Volume of Fluid (VOF) to simulate multiphase flows in OpenFOAM. The VOF method is one of the most widely used technique for tracking the interface between air and water and is often used for describing free surface flows. Therefore, the VOF method has been utilised in order to account for the free surface that is present within the flume. Turbulence modelling was achieved via the use of the k-ω SST model.

Two sets of simulations have been conducted: a single phase simulation solved with the time dependent solver pimpleFoam and a multiphase simulation solved with interFoam. Both simulations use the flow conditions found in Experiment 3 in Table 1. The single phase simulations employ a slip boundary at the top of the domain in order to closely replicate experiment. The multiphase simulations account for both water and air phases with an interface separating them. The main motivation for this comparison was to investigate the Froude number effect on the flow field found around the pier and to deduce its potential effect on scouring at the piers base. The fluid domain is a complete replica of the experimental flume's geometry. This ensured continuity between both experiment and numerical modelling and facilitated direct comparisons. A fully structured mesh consisting of 8 million and 15 million cells, respectively, is used throughout both simulations.

3.2 Model validation

Four locations of interest around the pier were selected in order to investigate how the free surface affects the flow field. As an auxiliary effect the turbulence models effectiveness in capturing the shearing of the flow around the pier was also investigated. Point 1 denotes the upstream location, this was used to establish identical velocity profiles ensuring the inlet conditions were similar for both experiment and simulation. Point 2 is located 50 mm upstream of the pier. Point 3 and 4 are both located 35 mm from the pier, the location of which can be found in Figure 5.

The average streamwise velocities are sampled over the whole depth of the flow and are compared with those results recorded by the ADV, the results of which can be found in Figure 6. The y coordinate i.e. distance from the bed is normalised by the piers diameter and the streamwise velocities are normalised by the free stream velocity.

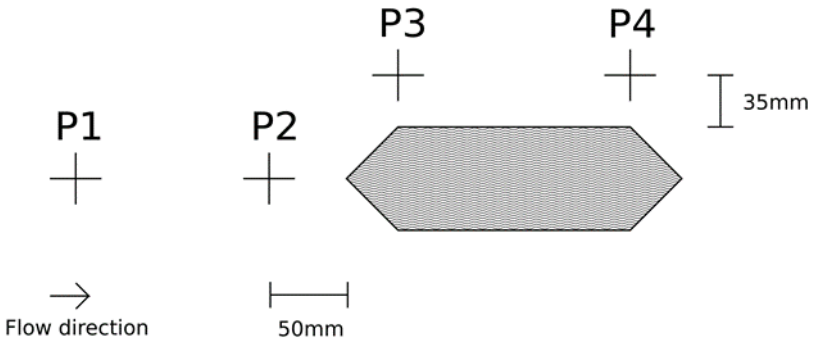

Figure 5. Location of sampling lines in CFD simulations.

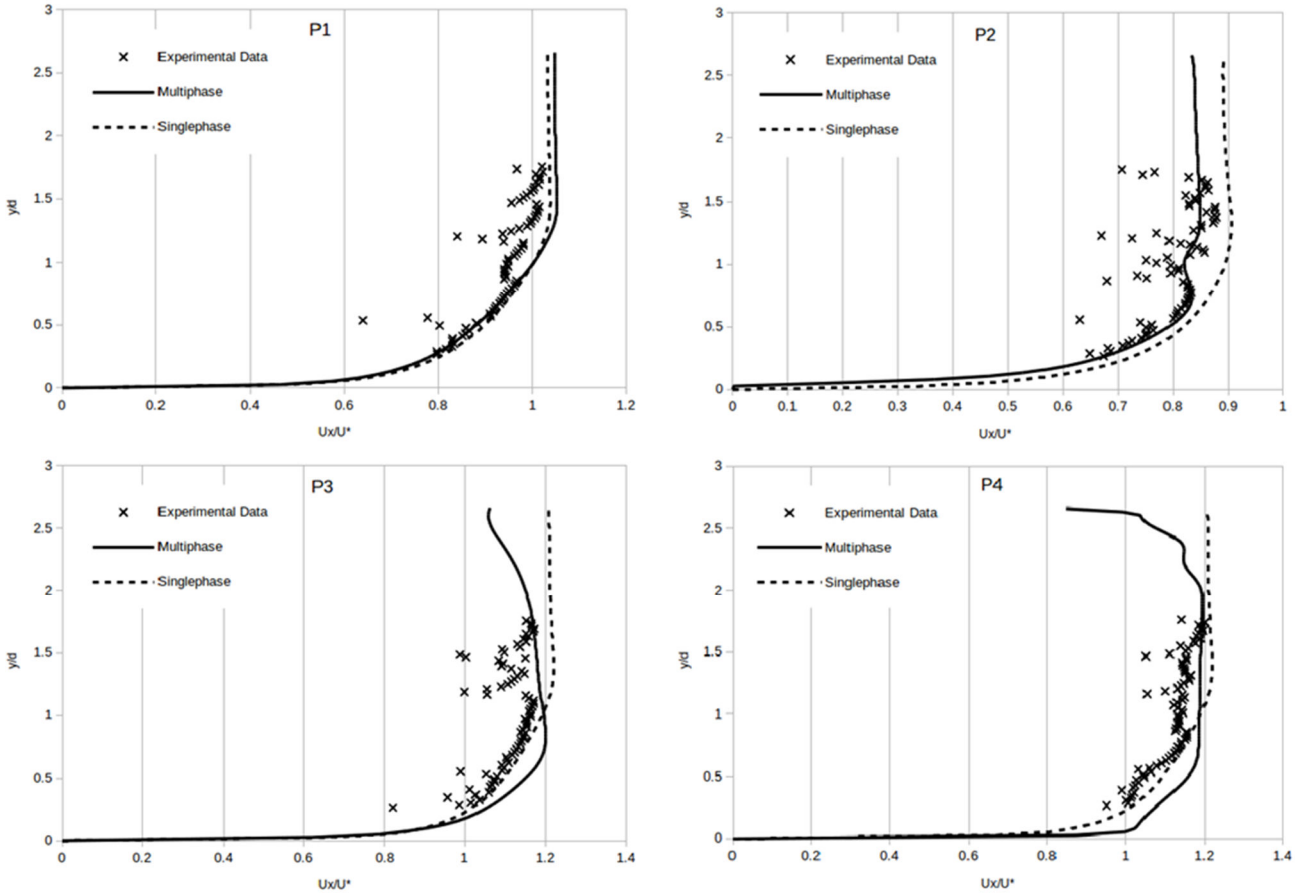

Figure 6. Normalised streamwise mean velocity profiles at four locations around the pier.

Looking at P1 it can be seen that the velocity profile is in good agreement for both simulations with the experimental data. There is a good match across the whole profile showing that the approach flow has been accurately captured by the simulation. P2 highlights the effect the free surface has on the velocity profile, in contrast to the single phase simulation the velocities are noticeably retarded showing differences up to 12%. The boundary layer has been captured in very good agreement with the experimental data. In this flow configuration a bulge is often present at the free surface often called a 'surface roller' this phenomenon is present within the model and is retarding the flow field across the depth of the flow.

P3's location is of great interest as this is the area in which the Froude number has its greatest effect. Looking at Figure 7, the surface jump is shown as the gravity forces begin to dominate the approach flows velocity. This phenomenon is present solely due to the hydrodynamics caused by the pier's geometry. There is a global increase in velocity as the flow is driven around the pier, the surface jump feeds into this process skewing the profile near the bed. Behaviour that isn't present within the single phase simulation, although it can be seen that the single phase simulation is in better agreement in this area suggesting that the free surface effect is being overestimated.

Finally, P4 shows good qualitative agreement with experiment, especially in the multiphase simulation. The simulations overestimate the velocities shown in the experimental data but the overall behaviour is captured. It is evident from these results that the free surface effects have a large impact on the immediate flow field found around the pier.

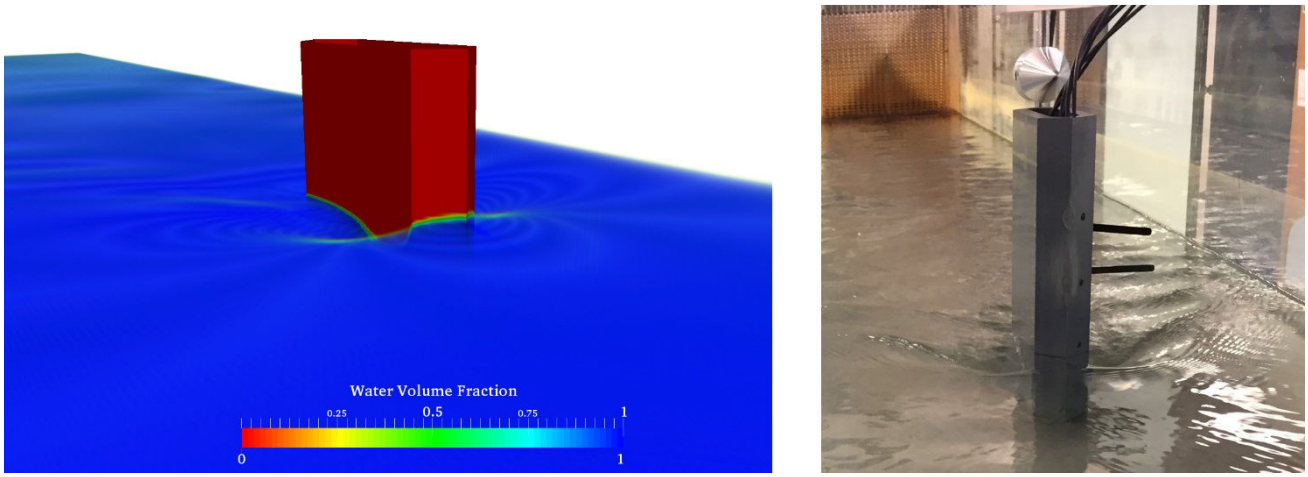

Figure 7. Free surface elevation around pier.

4 FUTURE RESEARCH

4.1 Flume experiments

Future experimental research will investigate scour at single span arch bridges due to debris blockage and the effects of various debris geometries such as a realistic tree trunk with rootwads. The project will also measure hydrodynamic pressures and forces using pressure sensors and load cells respectively. To the extent that time restrictions allow, effect of unsteady discharge and sediment grain diameter will also be investigated.

4.2 CFD simulations

Results from CFD simulations that for this geometry free surface effects are important even at relatively low Froude number. Although standard guidelines suggest a Froude number of less than 0.2 (Roulund et al. 2005) to omit the use of a free surface this facility is highly desirable. In an effort to predict real life conditions i.e. flooding this constraint is never going to be satisfied, also with the implementation of debris models the effect this has on the free surface is of great importance.

Building on these baseline simulations, the debris models will be implemented and solved with interFoam in order to account for the free surface. These will be compared directly with experimental results for further validation of the CFD models. Later the hydrodynamic effects of complex debris accumulations that are out of the scope of the experimental work such as block accumulations will be explored using CFD. The effect of Froude number on the free surface drop around the frontal corners of the pier will be explored to deduce how flooding conditions can exacerbate the scouring process.

A multiphase scour model will be developed which will run alongside interFoam. This will enable scour simulations in which the experimental data gathered in the flume can be directly compared and will enable validation.

5 CONCLUSIONS

Main findings of the present work are as following.

- Debris increased downward flow velocities and thereby scour at the base of the pier.
- The results between experiment and multiphase simulations show good overall agreement with an error estimated to be less than 10%.
- The Froude number of the flow has a large effect on the immediate flow field.
- From the baseline simulations the free surface has been effectively captured via the VOF method.

ACKNOWLEDGMENTS

The research presented in this paper was supported by funding from the UK's Engineering and Physical Sciences Research Council (EPSRC) under grant EP/M017354/1. For further information please refer to the project blog at http://blogs.exeter.ac.uk/ramb/ .

REFERENCES

Arneson, L.A., Zevenbergen, L.W., Lagasse, P.F. and Clopper, P.E., 2012. *Evaluating scour at bridges* (No. FHWA-HIF-12-003).

Beechie, T.J. and Sibley, T.H., 1997. Relationships between channel characteristics, woody debris, and fish habitat in northwestern Washington streams. *Transactions of the American Fisheries Society*, *126*(2), pp.217-229.

Benn, J., 2013. Railway bridge failure during flooding in the UK and Ireland. *Proceedings of the Institution of Civil Engineers-Forensic Engineering*, *166*(4), pp.163-170.

Bradley, J.B., Richards, D.L. and Bahner, C.C., 2005. *Debris control structures: Evaluation and countermeasures*. US Department of Transportation, Federal Highway Administration.

Bridle, R.J. and Sims, F. 2009. The effect of bridge failures on UK technical policy and practice. *Proceedings of the Institution of Civil Engineers - Engineering History and Heritage* 162(1): 39-49.

Chang, F.F. and Shen, H.W., 1979. *Debris problems in the river environment* (No. FHWA-RD-79-62 Final Rpt.).

Chanson, H., 2004. *Hydraulics of open channel flow*. Butterworth-Heinemann.

Comiti, F., Andreoli, A., Lenzi, M.A. and Mao, L., 2006. Spatial density and characteristics of woody debris in five mountain rivers of the Dolomites (Italian Alps). *Geomorphology*, *78*(1), pp.44-63.

Devon County Council (2015). Meeting with Kevin Dentith on 25 August 2015 at Devon County Council, Exeter, UK.

Diehl, T.H., 1997. *Potential drift accumulation at bridges*. US Department of Transportation, Federal Highway Administration, Research and Development, Turner-Fairbank Highway Research Center.

Ebrahimi, M., Kripakaran, P., Djordjević, S., Tabor, G., Kahraman, R., Prodanović, D. and Arthur, S. (2016). Hydrodynamic Effects of Debris Blockage and Scour on Masonry Bridges: Towards Experimental Modelling. *Proceedings of 8th International Conference on Scour and Erosion*. Oxford, UK.

Ettema, R., Melville, B.W. and Barkdoll, B., 1998. Scale effect in pier-scour experiments. *Journal of Hydraulic Engineering*, *124*(6), pp.639-642.

Frostick, L.E., McLelland, S.J. and Mercer, T.G. ed., 2011. *Users guide to physical modelling and experimentation: Experience of the HYDRALAB network*. CRC Press.

Highways Agency. 2012. The assessment of scour and other hydraulic actions at highway structures. In *Highways Agency, Design manual for roads and bridges*, vol 3, section 4, Part 21, BD 97/12. London.

Hjulström, F., 1939. Transportation of detritus by moving water: Part 1. Transportation.

Kail, J., 2003. Influence of large woody debris on the morphology of six central European streams. *Geomorphology*, *51*(1), pp.207-223.

Kamphuis, J.W., 1974. Determination of sand roughness for fixed beds. *Journal of Hydraulic Research*, *12*(2), pp.193-203.

Kirby, A.M, Roca, M., Kitchen, A., Escarameia, M. and Chesterton, O.J. 2015. *Manual on scour at bridges and other hydraulic structures,* second edition (Vol. C742). London: CIRIA.

Lagasse, P.F., Clopper, P.E., Zevenbergen, L.W., Spitz, W.J. and Girard, L.G. 2010. *Effects of debris on bridge pier scour* (Vol. 653). Transportation Research Board.

Laursen, E.M. and Toch, A., 1956. *Scour around bridge piers and abutments* (Vol. 4). Ames, IA: Iowa Highway Research Board.

Magilligan, F.J., Nislow, K.H., Fisher, G.B., Wright, J., Mackey, G. and Laser, M., 2008. The geomorphic function and characteristics of large woody debris in low gradient rivers, coastal Maine, USA. *Geomorphology*, *97*(3), pp.467-482.

May, R.W.P., Ackers, J.C. and Kirby, A.M., 2002. *Manual on scour at bridges and other hydraulic structures* (Vol. 551). London: CIRIA.

McKibbins, L.D., Melbourne, C., Sawar, N. and Gaillard, S.C. 2006. *Masonry arch bridges: condition appraisal and remedial treatment* (Vol. C656). London: CIRIA.

Melville, B.W. and Chiew, Y.M., 1999. Time scale for local scour at bridge piers. *Journal of Hydraulic Engineering*, *125*(1), pp.59-65.

Melville, B.W. and Dongol, D.M., 1992. Bridge pier scour with debris accumulation. *Journal of Hydraulic Engineering*, *118*(9), pp.1306-1310.

Pagliara, S. & Carnacina, I., 2011. Influence of large woody debris on sediment scour at bridge piers. *International Journal of Sediment Research*, 26(2), pp.121-136.

Pagliara, S. & Carnacina, I. 2013. Bridge pier flow field in the presence of debris accumulation. *Proceedings of the Institution of Civil Engineers-Water Management* (Vol. 166, No. 4, pp. 187-198).

Parola, A.C. Apeldt, C.J. and Jempson, M.A. 2000. Debris forces on highway bridges (No. 445). Transportation Research Board.

RAIB 2010. *Failure of Bridge RDG1 48 (River Crane) between Whitton and Feltham 14 November 2009*. Derby, UK.

Raudkivi, A.J. and Ettema, R. 1983. Clear-water scour at cylindrical piers. *Journal of Hydraulic Engineering*, 109(3), pp.338-350.

Roulund, A., Sumer, B.M., Fredsøe, J. and Michelsen, J., 2005. Numerical and experimental investigation of flow and scour around a circular pile. *Journal of Fluid Mechanics*, *534*, pp.351-401.

RSSB 2005. *Safe Management of Railway Structures, Phase 1: Flooding & Scour Risk*. London.

van Rijn, L.C., 1993. *Principles of sediment transport in rivers, estuaries and coastal seas* (Vol. 1006). Amsterdam: Aqua publications.

Wallerstein, N.P., Arthur, S. and Sisinngghi, D., 2010. Towards predicting flood risk associated with debris at structures. In *Proceedings of the IAHR APD conference 2010*.

Yalin, M.S. 1992. River Mechanics, Pergamon Press, Oxford.

Yalin, M.S. and da Silva, A.M.F. 2001. Fluvial Processes, IAHR Monograph, IAHR, Delft.